POLITECNICO DI TORINO
Repository ISTITUZIONALE

Blind modulation format identification for digital coherent receivers

Original
Blind modulation format identification for digital coherent receivers / Bilal, S.M., Bosco, G., Dong, Z., Lau, A.P.T., Lu, C.. - In: OPTICS EXPRESS. - ISSN 1094-4087. - ELETTRONICO. - 23:20(2015), pp. 26769-26778. [10.1364/OE.23.026769]

Availability:
This version is available at: 11583/2645926 since: 2016-08-03T14:15:16Z

Publisher:
OSA - The Optical Society

Published
DOI:10.1364/OE.23.026769

Terms of use:

This article is made available under terms and conditions as specified in the corresponding bibliographic description in the repository

Publisher copyright

(Article begins on next page)

26 June 2026

Blind modulation format identification for digital coherent receivers

Syed Muhammad Bilal,[1,*] Gabriella Bosco,[1] Zhenhua Dong,[2] Alan Pak Tao Lau,[2] and Chao Lu[2]

[1]*DET, Politecnico di Torino, Corso Duca degli Abruzzi*, 24, 10129, *Torino, Italy*
[2]*Photonics Research Center, The Hong Kong Polytechnic University, Hong Kong, China*
[*]*bilalsyedm@gmail.com*

Abstract: In this paper, a simple novel digital modulation format identification (MFI) scheme for coherent optical systems is proposed. The scheme is based on the evaluation of the peak-to-average-power ratio (PAPR) of the incoming data samples after analog-to-digital conversion (ADC), chromatic dispersion (CD) and polarization mode demultiplexing (PMD) compensation at the receiver (Rx). Since at a particular optical-signal-to-noise ratio (OSNR) value different modulation formats have distinct PAPR values, it is possible to identify them. The proposed scheme and the results are analyzed both experimentally and through numerical simulations. The results demonstrate successful identification among four modulation formats (MF) commonly used in digital coherent systems.

© 2015 Optical Society of America

OCIS codes: (060.1660) Coherent communications; (060.4080) Modulation; (060.2360) Fiber optics links and subsystems.

References and links

1. Cisco Visual Networking Index: Forecast and Methodology, 2013–2018. [Online] Available at (http://www.cisco.com/en/US/solutions/collateral/ns341/ns525/ns537/ns705/ns827/white_paper_c11-481360.pdf).
2. A. Nag, M. Tornatore, and B. Mukherjee, "Optical network design with mixed line rates and multiple modulation formats," J. Lightwave Technol. **28**(4), 466–475 (2010).
3. J. Mitola III, "Software radios-survey, critical evaluation and future directions," in *Telesystems Conference*, NTC-92 (1992).
4. K. Roberts and C. Laperle, "Flexible transceivers," in *European Conference and Exhibition on Optical Communication*, paper. We.3.A.3 (2012).
5. R. Borkowski, D. Zibar, A. Caballero, V. Arlunno, and I. T. Monroy, "Optical modulation format recognition in stokes space for digital coherent receivers," in *Optical Fiber Communication Conference/National Fiber Optic Engineers Conference* (OSA, 2013) paper. OTh3B.3.
6. O. Dobre, A. Abdi, Y. Bar-Ness, and W. Su, "Survey of automatic modulation classification techniques: classical approaches and new trends," IET Communications **1**(2), 137–156 (2007).
7. F. N. Khan, Y. Zhou, A. P. T. Lau, and C. Lu, "Modulation format identification in heterogeneous fiber-optic networks using artificial neural networks," Opt. Express **20**(11), 12422–12431 (2012).
8. N. Gonzalez, D. Zibar, and I. Monroy, "Cognitive digital receiver for burst mode phase modulated radio over fiber links," in *European Conference and Exhibition on Optical Communication*, paper. P6.11 (2010).
9. J. Liu, Z. Dong, K. P. Zhong, A. P. T. Lau, C. Lu, and Y. Lu, "Modulation format identification based on received signal power distributions for digital coherent receivers," in *Optical Fiber Communication Conference/National Fiber Optic Engineers Conference* (IEEE, 2014), paper. Th4D.3.
10. E. Adles, M. Dennis, W. Johnson, T. McKenna, C. Menyuk, J. Sluz, R. Sova, M. Taylor, and R. Venkat, "Blind optical modulation format identification from physical layer characteristics," J. Lightwave Technol. **32**(8), 1501–1509 (2014).
11. Z. Dong, A. P. T. Lau, and C. Lu, "OSNR monitoring for QPSK and 16-QAM systems in presence of fiber nonlinearities for digital coherent receivers," Opt. Express **20**(17), 19520–19534 (2012).

#245649 Received 14 Jul 2015; revised 4 Sep 2015; accepted 5 Sep 2015; published 2 Oct 2015
© 2015 OSA

12. C. Zhu, A. V. Tran, S. Chen, L. B. Du, C. C. Do, T. Anderson, A. J. Lowery, and E. Skafidas, "Statistical moments-based OSNR monitoring for coherent optical systems," Opt. Express **20**(16), 17711–17721 (2012).
13. Z. Dong, K. Zhong, X. Zhou, C. Lu, A. Lau, Y. Lu, and L. Li, "Modulation-format-independent OSNR monitoring insensitive to cascaded filtering effects by low-cost coherent receptions and RF power measurements," Opt. Express **23** (12), 15971–15982 (2015).
14. S. Oda, Jeng-Yuan Yang, Y. Akasaka, K. Sone, Y. Aoki, M. Sekiya, and J. C. Rasmussen, "In-band OSNR monitor using an optical bandpass filter and optical power measurements for superchannel signals," in *European Conference and Exhibition on Optical Communication* (IEEE, 2013) paper. P.3.12.
15. S. M. Bilal, C. Fludger, V. Curri, and G. Bosco, "Multi-stage CPE algorithms for phase noise mitigation in 64-QAM optical systems," J. Lightwave Technol. **32**(17), 2973–2980 (2014).

1. Introduction

Annual global IP traffic is predicted to increase by almost threefold over the next 5 years and will cross the zettabyte (10^{21} bytes) threshold in 2016 [1]. This presents a big challenge to the current and future optical networks and hence requires flexible transceivers supporting mixed data rates and multiple modulation formats [2]. The model of flexible optical transceivers is based on the software defined radios (SDRs) of wireless that allows the system to be reconfigured in software for implementing the most suitable transmission protocol [3]. This makes the optical transmitter and receiver *'software-programmable'* and allows them to configure various transmission schemes by implementing different data rates, modulation formats and forward error correction (FEC) protocols [4].

Owing to the flexible transceivers, it is no longer guaranteed that the signals arriving at the receiver side would have the same, known in advance, modulation format (MF) [5]. The receiver thus needs to have some *'blind'* or *'flexible'* algorithms to adapt to these changes. Modulation format identification (MFI) is of high interest for the next generation fiber-optic networks as it could grant more autonomy and flexibility to the network. Elastic optical networks (EON) and cognitive optical networks (CON), with rate-adaptive transceivers [4] supporting multiple modulation formats, have recently drawn a considerable interest as future optical networks.

Although MFI for wireless systems has been thoroughly investigated [6], not much work has been done for the recognition/identification of modulation formats in fiber-optic networks. For MFI, a digital coherent receiver should be able to identify the MF of the incoming signals to ensure proper demodulation. However in optical communication systems frequency offset compensation (FOC) and carrier phase estimation (CPE) techniques require a prior knowledge of the modulation format. This makes blind MFI on-the-fly more difficult.

Up till now very few techniques are available in the literature for blind MFI. Some are based on artificial neural networks [7], Expectation-Maximization (EM) [5] and k-means clustering [8], and require very complex iterative algorithms, while others are based on received signal power distribution [9] and physical-layer signal characteristics [10] and have high algorithmic complexity.

In this paper we propose a simple and novel MFI scheme based on the evaluation of the peak-to-average-power ratio (PAPR) of the received data samples. At a particular optical signal to noise ratio (OSNR) value, different modulation formats have distinct PAPR which can be used as defining parameter for their correct identification. Simulation and experimental results demonstrate successful identification of four commonly used modulation formats. Furthermore, the proposed technique can also be extended to other lower or higher order formats.

2. Modulation format identification (MFI) scheme

The MFI scheme is based on two steps which are described in the following:

1) Blind OSNR monitoring

2) Evaluation of PAPR at that OSNR value

#245649 Received 14 Jul 2015; revised 4 Sep 2015; accepted 5 Sep 2015; published 2 Oct 2015
© 2015 OSA

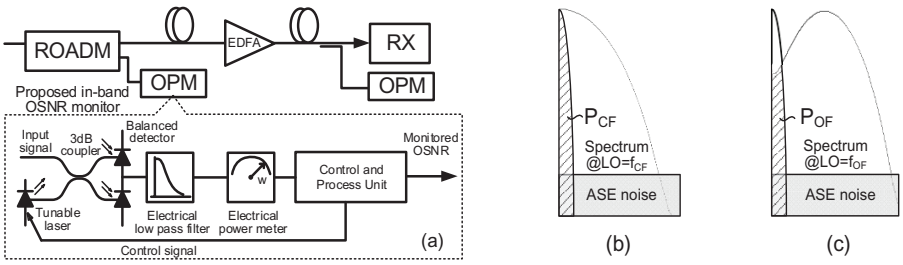

Fig. 1. (a) Schematic diagram of proposed in-band OSNR monitor, (b)-(c) RF spectra after balanced detector showing filtered signal and ASE noise, whereas P_{CF} and P_{OF} represent the electrical power of centrally filtering f_{CF} and offset filtering at frequency f_{OF}.

2.1. Blind OSNR Monitoring

Several techniques are available in the literature for blind OSNR monitoring [11–14]. We have adopted a recently proposed in-band OSNR monitoring scheme [13] for our MFI technique. Figure 1(a) shows the schematic diagram of the proposed in-band OSNR monitor deployed at the intermediate network nodes which consists of a tunable laser, a 3 dB coupler, a low speed balance detector, a low pass electrical filter, an electric power meter and a control and process unit (CPU). First, the incoming signal tapped from the transmission link is mixed and beaten with a continuous light produced by the tunable laser though a 3 dB coupler and a balance detector. The input signal is coherently received and the obtained baseband RF signal is then filtered out by the electrical low pass filter. By tuning the frequency of tunable laser to the central frequency of the target channel f_{CF}, and the offset frequency f_{OF}, the power of the target optical signal at two different frequencies are converted to the correspond electric power and are measured by the electrical power meter as P_{CF} and P_{OF} respectively (See Fig. 1(b)-(c)). The relationship among P_{CF}, P_{OF}, signal power (P_{SIG}) and amplified spontaneous emission (ASE) noise power (P_{ASE}) can be described as [13]:

$$P_{CF} = P_{SIG} + P_{ASE}, \qquad P_{OF} = RP_{SIG} + P_{ASE} \tag{1}$$

where the amount of ASE noise at f_{CF} and f_{OF} is assumed to be the same. The calibration parameter R can be obtained by placing the monitor at the Tx-side and performing a back to back measurement where the ASE noise is negligible, i.e. R=P_{OF-Tx}/P_{CF-Tx}. Then in the CPU the monitored OSNR can be calculated as:

$$OSNR = \gamma \frac{P_{SIG}}{P_{ASE}} = \gamma \frac{1 - P_{CF}/P_{OF}}{(P_{CF}/P_{OF})R - 1} \tag{2}$$

where the calibration parameter γ is determined by the relationship among the electrical filter bandwidth, signal bandwidth and defined noise bandwidth and can be obtained by a back to back measurement. Using this scheme successful monitoring of OSNR was obtained within 1 dB error. However, it is important to note that the OSNR monitoring will be a very difficult task in the high spectral efficiency transmission systems due to the limited guard-band between sub-channels.

2.2. PAPR evaluation

After getting an OSNR value the next step is the evaluation of PAPR after analog to digital conversion (ADC), chromatic dispersion (CD) compensation and polarization demultiplexing.

#245649 Received 14 Jul 2015; revised 4 Sep 2015; accepted 5 Sep 2015; published 2 Oct 2015
© 2015 OSA

The PAPR is defined as:

$$\text{PAPR} = max_k \frac{|y_k|^2}{P_{av}} \tag{3}$$

where P_{av} is the average power and y_k are the equalized received data samples affected by both additive Gaussian noise (AGN) and phase noise. They can be written as:

$$y_k = x_k e^{j\theta_k} + n_k \tag{4}$$

where x_k are data symbols which can be QPSK, 16-QAM, 64-QAM or 256-QAM. n_k is the additive white Gaussian noise (AWGN), which models the ASE noise introduced by optical amplifiers. The laser phase noise θ_k is modeled as a Wiener process [15] in which

$$\theta_k = \sum_{i=-\infty}^{k} v_i \tag{5}$$

where v_i's are independent and identically distributed Gaussian random variables with zero mean and variance

$$\sigma_f^2 = 2\pi\Delta\nu \cdot T_s \tag{6}$$

where $\Delta\nu$ is the laser linewidth and T_s is the symbol period.

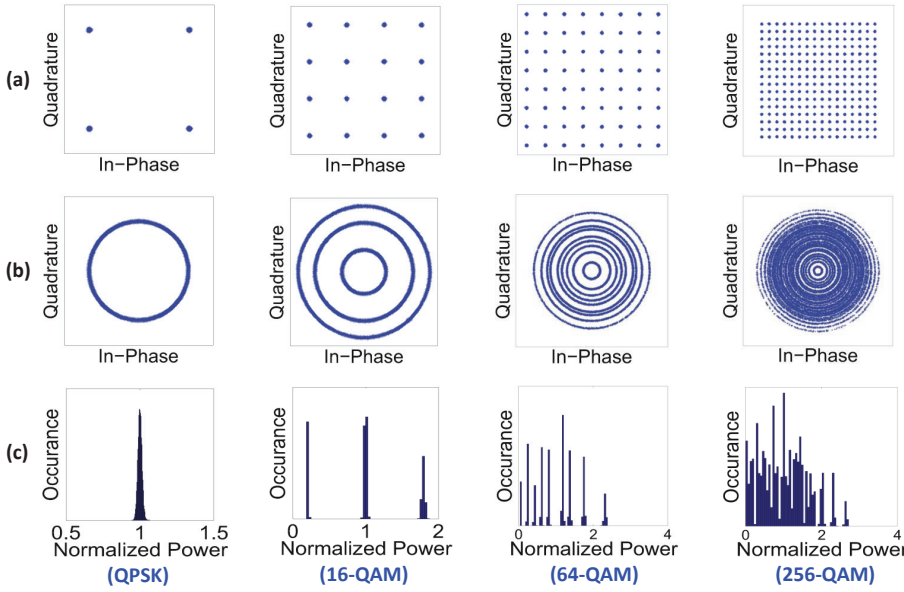

Fig. 2. (a) Constellations, (b) Received signals in presence of frequency offset, phase noise and other impairments, (c) Normalized signal power distributions.

If we normalize the data samples so that their average power is the same, the only quantity to be considered in the PAPR evaluation will be the peak power (PP). Figure 2(a) shows the constellation plot of QPSK, 16-QAM, 64-QAM and 256-QAM. Figure 2(b) shows the same constellations affected by frequency offset, phase noise and other impairments. Figure 2(c) shows the distribution of the normalized power samples with different PP values for different modulation formats. Higher the order of the QAM modulation format, higher will be its PP (provided that P_{av} is the same). At different OSNR values, PAPR of different modulation formats have distinct values and hence can be used for MFI.

#245649 Received 14 Jul 2015; revised 4 Sep 2015; accepted 5 Sep 2015; published 2 Oct 2015
© 2015 OSA

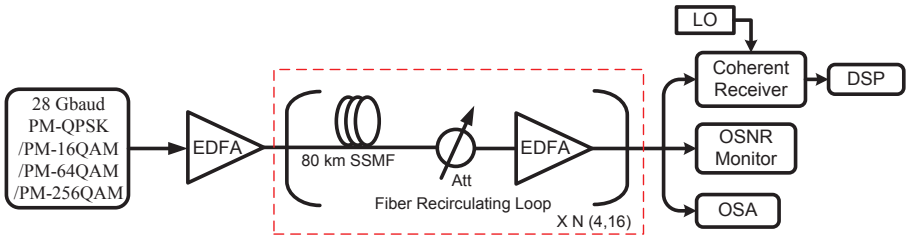

Fig. 3. Simulation Setup.

3. Simulation setup and results

The simulation setup for in-band OSNR monitoring and PAPR evaluations for MFI is shown in Fig. 3. Four polarization-multiplexed (PM) modulation formats (PM-QPSK, PM-16QAM, PM-64QAM and PM-256-QAM) at 28 Gbaud are generated at the transmitter side. The transmitter laser (Tx) is set to 1553.12 nm and has a linewidth of 100 kHz. The resulting signal is then amplified by an erbium-doped fiber amplifier (EDFA) and transmitted through a recirculating loop which consists of 80-km standard single-mode fiber (SSMF) and an EDFA. The EDFA inside the loop fully compensates for the span loss. A tunable attenuator is placed before the EDFA to set the OSNR values for the received signals. At the loop output, the signal is simultaneously received by a coherent receiver (LO linewidth 100 kHz), an OSNR monitor and an optical spectrum analyzer (OSA) for comparison. The reference OSNR measured by OSA uses out-of-band noise measurement and refers to 0.1 nm noise bandwidth [11]. In-band OSNR monitor blindly monitors the OSNR (within 1 dB error) whereas the coherently detected samples enter the digital signal processing (DSP) unit. For back-to-back analysis, the portion enclosed by red dashed rectangle in Fig. 3 is omitted and is replaced by an attenuator. The tunable attenuator is used to set the OSNR values for the received signals.

The curves in Figs. 4 and 5 show the simulation results for a back-to-back system in terms of the mean (μ_{PAPR}) and standard deviation (σ_{PAPR}) of the estimated PAPR values as a function of OSNR for the four modulation formats, respectively. The values of μ_{PAPR} and σ_{PAPR} for each modulation format and each OSNR value have been obtained by evaluating, respectively, the average and the standard deviation of the PAPR values estimated running $10,000$ Monte-Carlo simulations. The PAPR values have been evaluated by considering an increasing number of symbols (from 10,000 in Figs. 4(a) and 5(a) to 100,000 in Figs. 4(d) and 5(d)). The number of considered symbols has been varied to asses the sensitivity of the proposed scheme to the length of the estimation window. In Fig. 4 black dashed curves, which show the threshold value at a particular OSNR, are also shown. These curves are obtained by taking the average of the μ_{PAPR} values between two neighboring modulation formats.

The curves in Fig. 6 show the the average PAPR values as a function of OSNR for the four modulation formats after propagation. Solid and dotted lines in Fig. 6 are for 320 km (4-loops) and 1280 km (16-loops) fiber systems, respectively. The fiber length was varied to check the performance of the proposed algorithm against fiber non-linearities (0 dBm input signal power) and different transmission configurations. Approximately 2^{17} symbols are used for PAPR evaluations.

The received signals are sampled at 2 samples per symbol (SpS) and processed off-line through different stages of a digital signal processing (DSP) unit, as shown in the right part of Fig. 7. The PAPR scheme for MFI is introduced after modulation format independent constant modulus algorithm (CMA) used for polarization demultiplexing (see Fig. 7). For CMA equalization a 21 taps filter and an step size of 10^{-4} was used. Note that before introducing the

#245649 Received 14 Jul 2015; revised 4 Sep 2015; accepted 5 Sep 2015; published 2 Oct 2015
© 2015 OSA

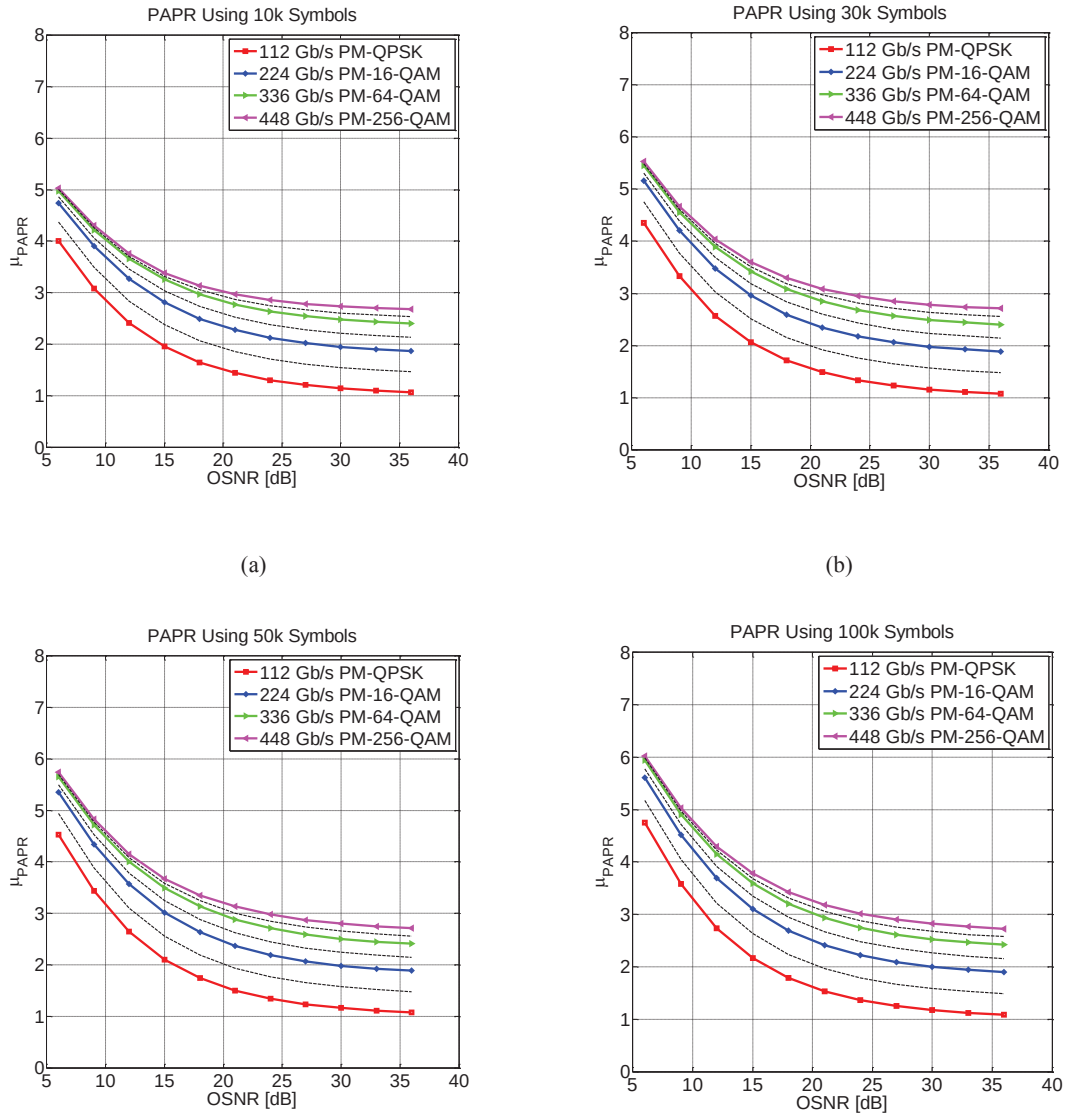

Fig. 4. Mean values of estimated PAPR (μ_{PAPR}) vs OSNR for different modulation formats and different number of symbols used in the PAPR estimation.

#245649 Received 14 Jul 2015; revised 4 Sep 2015; accepted 5 Sep 2015; published 2 Oct 2015
© 2015 OSA

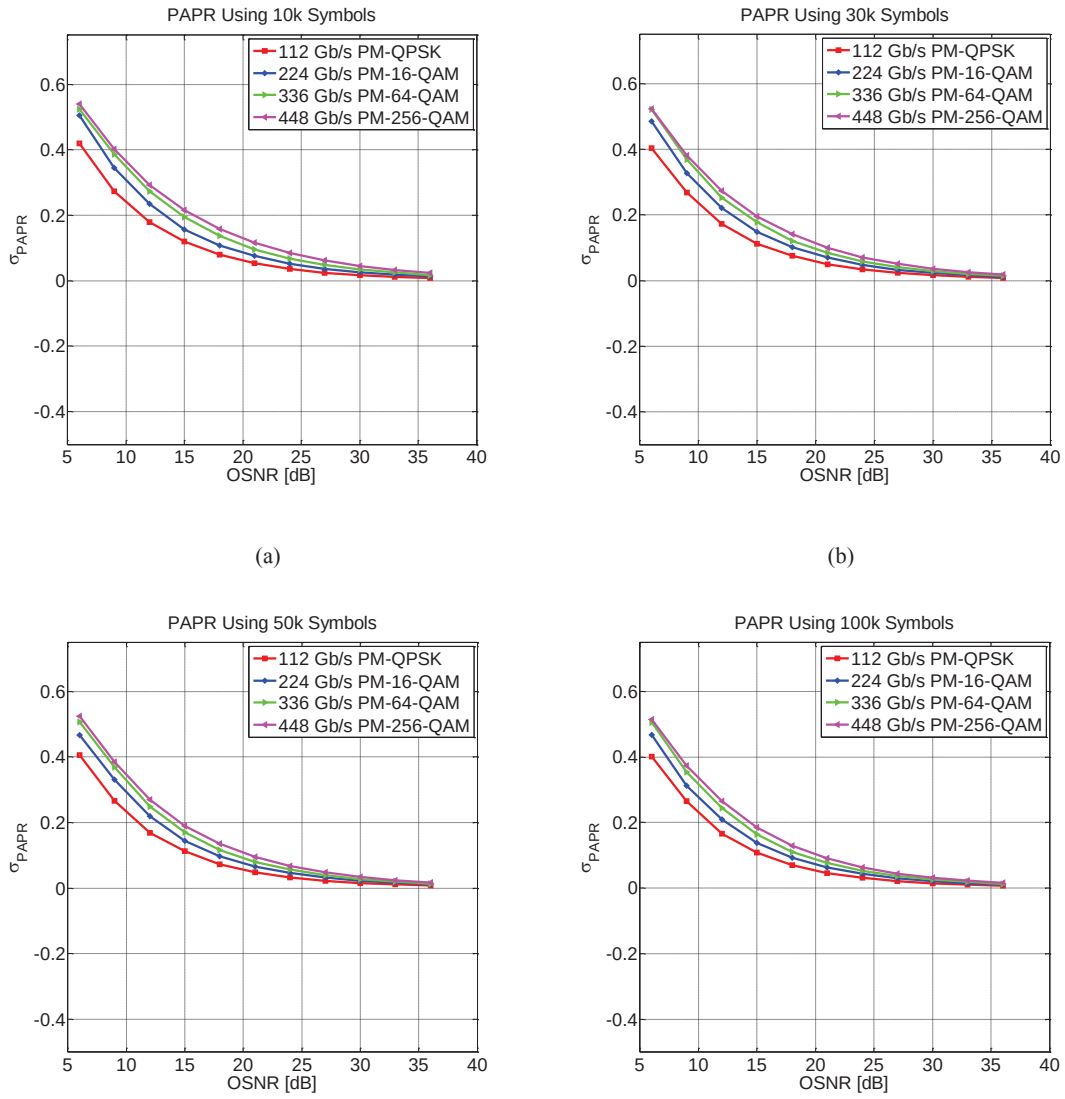

Fig. 5. Standard deviation of estimated PAPR (σ_{PAPR}) vs OSNR for different modulation formats and different number of symbols used in the PAPR estimation.

#245649 Received 14 Jul 2015; revised 4 Sep 2015; accepted 5 Sep 2015; published 2 Oct 2015
© 2015 OSA

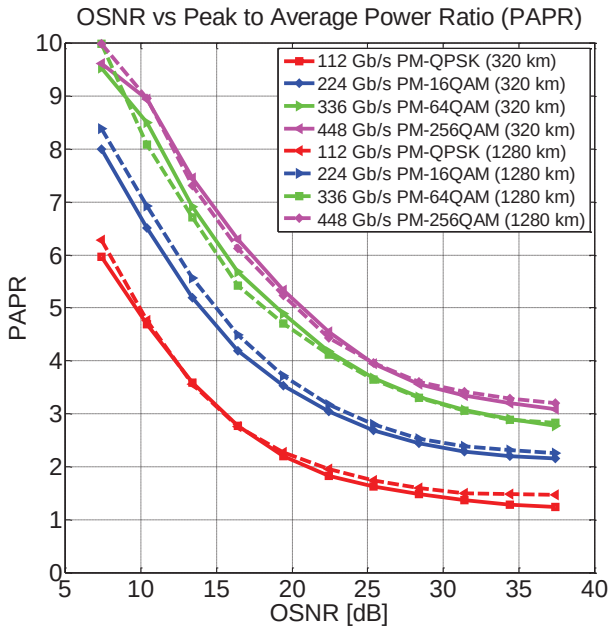

Fig. 6. Simulation results for polarization multiplexed (PM) QPSK, 16-QAM, 64-QAM and 256-QAM systems at 28 Gbaud for different fiber lengths.

MFI scheme all the other schemes in Fig. 7 i.e normalization and resampling, CD compensation and CMA are all modulation format independent. Since the proposed scheme is applied after CMA equalization, it is also independent of the pulse shape.

The simulation results shown in Figs. 4 and 6 indicate that successful MFI can be obtained at different symbol and fiber lengths, respectively, indicating that the proposed technique is independent of number of symbols used for PAPR evaluation, fiber non-linearities and transmission length. At a particular OSNR, a threshold (indicated by black dashed curves in Fig. 4) can be used for successful MFI between different modulation formats.

The plots in Figs. 4 and 6 show that the curves get closer in low OSNR region, making MFI somewhat difficult. This is because ASE noise is very high at low OSNR values and hence can significantly affect the PAPR. However, each modulation format with OSNR values in its normal operating region (BER $\approx 10^{-2}$, considering FEC threshold with 20% overhead) shows that a successful MFI can be obtained. Table 1 gives the theoretical OSNR values @ BER $\approx 10^{-2}$ for the considered modulation formats.

Table 1. Theoretical OSNR Values for Different Modulation Formats @ BER $\approx 10^{-2}$

Case	Modulation Format	OSNR @ BER $\approx 10^{-2}$ (dB)
1	PM-QPSK	7.3
2	PM-16QAM	13.9
3	PM-64QAM	19.7
4	PM-256QAM	25.4

#245649 Received 14 Jul 2015; revised 4 Sep 2015; accepted 5 Sep 2015; published 2 Oct 2015
© 2015 OSA

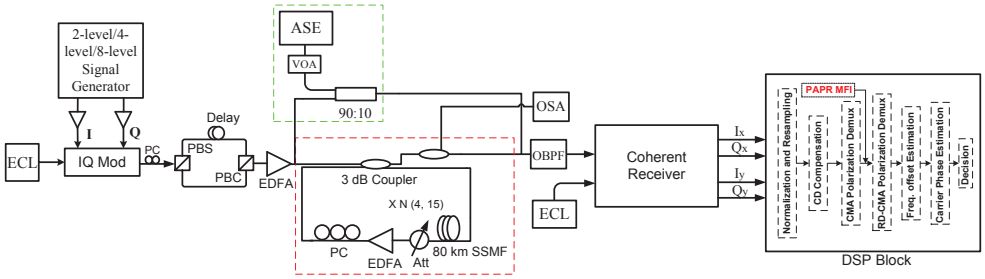

Fig. 7. Experimental Setup for modulation format identification (MFI) of 112 Gb/s (28GBaud) PM-QPSK, 112 Gb/s (14Gbaud) PM-16-QAM and 240 Gb/s (20Gbaud) PM-64-QAM systems.

4. Experimental setup and results

The experimental setup is shown in Fig. 7. An external cavity laser (ECL) with a linewidth of 100 kHz and wavelength 1550.32 nm is modulated by an integrated IQ modulator. The I and Q branches of the IQ modulator are driven by two 14-Gbaud 4-level and 20-Gbaud 8-level electrical signals in order to generate 16-QAM and 64-QAM signals, respectively. A 28-Gbaud 2-level signal generator is also included for generating PM-QPSK signals.

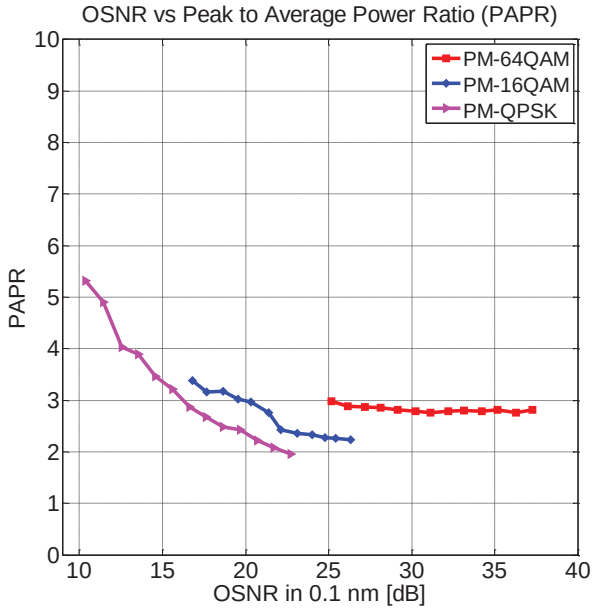

Fig. 8. PAPR vs OSNR for polarization multiplexed (PM) QPSK, 16-QAM and 64-QAM after CMA for a back to back system.

The modulated optical signal is then polarization multiplexed through polarization beam splitter (PBS), optical delay lines and polarization beam combiner (PBC). The resulting signal is then amplified by an erbium-doped fiber amplifier (EDFA) and transmitted through a fiber recirculating loop which consists of 80-km standard single-mode fiber (SSMF) and an EDFA. A tunable attenuator is placed before the EDFA to set the OSNR values for the received signals. At the receiver side, an optical band pass filter (OBPF) with bandwidth 0.6nm is used for filtering the out-band noise. The received signal is coherently detected by an integrated coherent

#245649 Received 14 Jul 2015; revised 4 Sep 2015; accepted 5 Sep 2015; published 2 Oct 2015
© 2015 OSA

receiver with a local oscillator (ECL, with line-width 100 kHz). The detected signal is sampled by a real-time sampling scope of 80 GS/s for 16QAM and 50 GS/s for the other two formats. The captured data is processed offline using DSP algorithms shown in Fig. 7. For back-to-back analysis, the portion enclosed by red dashed rectangle in Fig. 7 is omitted and is replaced by the portion enclosed by green dashed rectangle.

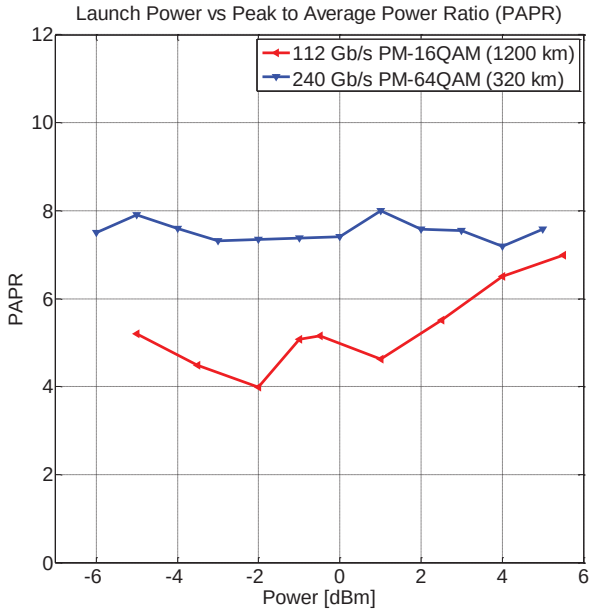

Fig. 9. PAPR vs Launch Power after CMA for 16-QAM(1200 km) and 64-QAM(320 km) fiber systems.

The PAPR evaluation block is introduced after the modulation format independent CMA stage used for polarization demultiplexing in the DSP unit for MFI, as shown in Fig. 7. The CMA for polarization demultiplexing consists of two stages. The 1st stage is the conventional modulation format independent CMA while the 2nd stage is the modulation-format-dependent radius-directed constant modulus algorithm (RD-CMA). The PAPR scheme for MFI is introduced after the 1st CMA stage.

Figure 8 shows the plot of PAPR vs OSNR whereas Fig. 9 shows the plot of PAPR vs Launch Power after modulation format independent CMA algorithm. Curves in Fig. 8 are for a back-to-back PM QPSK, 16-QAM and 64-QAM systems. Curves in Fig. 9 are for 1200 km (15-loops) 112 Gb/s PM 16-QAM and 320 km (4-loops) 240 Gb/s PM 64-QAM fiber systems. The experimental results shown in Figs. 8 and 9 after CMA are in good agreement with the simulation results. At each OSNR or launch power value, PAPR of different modulation formats have distinct values and hence can be used for MFI.

5. Conclusion

In this paper, a simple novel MFI scheme based on the evaluation of PAPR of the incoming data samples is proposed. To the best of our knowledge the scheme proposed here is the simplest among all the schemes present in the literature. By setting a threshold at a particular OSNR value, the technique can perform blind MFI on-the-fly for several optical modulation formats. The proposed technique was analyzed both experimentally and through numerical simulations obtaining a successful identification of multi-level QAM modulation formats.

#245649 Received 14 Jul 2015; revised 4 Sep 2015; accepted 5 Sep 2015; published 2 Oct 2015
© 2015 OSA